Gap junction-dependent amino acid transfer promotes germ cell growth

Caroline Vachias[1], Camille Tourlonias[1], Louis Grelée[1], Nathalie Gueguen[1], Yoan Renaud[1], Parvathy Venugopal[1], Graziella Richard[1], Pierre Pouchin[1], Émilie Brasset[1], Vincent Mirouse[1]*

1) Institute of Genetics, Reproduction and Development (iGReD), Université Clermont Auvergne - UMR CNRS 6293 - INSERM U1103, Faculté de Médecine, 28 Place Henri-Dunant, 63000 Clermont-Ferrand, France
*contact: vincent.mirouse@uca.fr

Abstract 180 words

Gap junctions allow the exchange of small molecules between cells. How this function could be used to promote cell growth has never been explored. During *Drosophila* ovarian follicle development, germ cells, which are surrounded by epithelial somatic cells, undergo massive growth. We found that this growth depends on gap junctions between these cell populations, with a requirement for Innexin4 and Innexin2, in the germ cells and the somatic cells, respectively. Somatic cells express enzymes and transporters involved in amino acid metabolism that are absent in germ cells. Among them, we identified a proline transporter required for germline growth. Its ectopic expression in the germline can compensate for its absence in somatic cells, confirming the metabolic exchange between these cell types. Moreover, in somatic cells, innexin2 expression and gap junction assembly are regulated by the insulin receptor/PI3K kinase pathway. Altogether these data illustrate how metabolic exchange through gap junctions can promote cell growth and how such mechanism can be integrated into a developmental programme, coupling growth control by extrinsic systemic signals with the intrinsic coordination between cell populations.

Key words

Drosophila, innexins, germ cells, metabolism, SLC36, P-bodies

Running title

Cell growth control by gap junctions

Summary statement between 15 and 30 words,

We demonstrate that gap junction-dependent metabolic flow from a cell population to another promotes cell growth and can be regulated to coordinate cell growth.

Introduction

Gap junctions are channels between adjacent cells. Each cells harbour a hemichannel made of six subunits, connexins in vertebrates and innexins in other animal phyla where gap junctions are found. These two protein families are very different in terms of primary sequence, but similar in terms of conformation (Bauer et al 2005; Evans 2015; Oshima et al 2016; Skerrett, & Williams 2017). Hemichannels can be homomeric or heteromeric in composition and channels can be formed from two identical or different hemichannels, leading to a large range of channel combinations with different regulations or solute specificities. Gap junctions generally assemble in plaques that contain many channels and each channel allows the direct communication, and thus molecular flows, between the cytoplasm of two cells. However, due to the channel size and conformation, only passive transfer of small molecules and ions, up to approximatively 1KDa, including second messengers (e.g. inositol triphosphate and calcium) is allowed. Gap junction proteins also participate in other cellular mechanisms, such as cell migration (Elias et al 2007; Miao et al 2020). Moreover, many molecules that can diffuse through gap junctions are linked to energetic metabolism (e.g. glucose and pyruvate) and to anabolic metabolism (e.g. amino acids). However, despite many studies on these metabolite flows, their functional relevance has been elusive.

Such metabolite exchanges could promote cell growth. Available genetic data suggest that the growth of mammalian oocytes could be an illustration of such a mechanism. Indeed, mutation of connexin 37 (*Cx37*) in germ cells or of *Cx43* in somatic granulosa cells, which surround and are in contact with the oocyte, strongly impairs oocyte and follicle growth (Gittens, & Kidder 2005; Simon et al 1997). Moreover, amino acid import and pyruvate production are more efficient in follicle cells, suggesting a potential metabolic flow towards the oocyte (Eppig et al 2005; Sugiura et al 2005). Nonetheless, it is not known: i) to which extent this putative transfer of metabolites contributes to explain gap junction impact on oocyte growth; and ii) whether such mechanism is coupled with follicle cell growth and more generally, is integrated in the genetic programme controlling follicle development.

A major feature of oocytes is their large size throughout animal evolution, despite important variation among species (Doherty et al 2022; Church et al 2019). Their size prefigures the early embryo size and their content will determine the early embryo development success rate and quality (Petkova et al 2014; Burn et al 2015). Hence, oocyte growth is an essential step that requires robust underlying mechanisms (Doherty et al 2021; Vachias et al 2014b). Oocyte development and growth usually occur in ovarian follicles where germ cells are surrounded by follicle cells (i.e. somatic epithelial cells). *Drosophila* oogenesis takes place in a structure called ovariole, in which follicles continuously arise and develop from the anterior to the posterior end. Each ovary is subdivided in about 16 ovarioles (Fig. 1A). Follicles bud from a structure called the germarium that contains germ cells and somatic stem cells. Follicle development is divided in 14

74 morphological stages during which the oocyte volume increases 1000 times in about 3 days
75 before being fertilized and laid (Spradling et al 1993). At stage 1, a follicle contains a germline cyst
76 of 16 interconnected cells: 15 nurse cells that will grow by endoreplication and 1 oocyte at the
77 posterior end, blocked in early meiosis. Each germline cyst is encapsulated by the follicular
78 epithelium that is initially composed of about 30 cells. These cells proliferate giving 800 cells at
79 stage 6 and then they undergo endoreplication (Chen et al 2019). Both germ cell growth and follicle
80 cell growth are cell autonomously sensitive to the usual growth systemic signals, such as the
81 Insulin Receptor/Phosphatidylinositol 3 Kinase (InR/PI3K) and Target of Rapamycin (TOR)
82 pathways (Drummond-Barbosa, & Spradling 2001; LaFever et al 2010; Sun et al 2010; Vachias et
83 al 2014b). These pathways affect also non-cell autonomously the growth of the adjacent tissue in
84 both direction: the soma influences germline growth and *vice versa* (LaFever et al 2010; Maines et
85 al 2004; Sun et al 2010; Vachias et al 2014b; Wang, & Riechmann 2007). The most striking
86 illustration of this reciprocal coordination is observed when *Pten*, a InR/PI3K repressor, is mutated
87 in follicle somatic cells. The faster growth of these somatic cells induces the faster growth of the
88 surrounded wild-type germ cells. Regulation of somatic cell growth by germline growth involves
89 the Hippo pathway and its modulation by tension induced on the epithelium due to the germline
90 cyst volume increase (Borreguero-Muñoz et al 2019). However, it is not known how the follicle
91 somatic cells control germ cell growth.
92 Here, we tested the hypothesis of an evolutionary conservation of gap junction function between
93 germ cells and follicle cells to regulate *Drosophila* female germ cell growth and explored the
94 underlying mechanism. Several reports indicate that gap junctions are present during fly
95 oogenesis. In gem cells, innexin 4 (Inx4) forms plaques at the contact with follicle cells (Tazuke et
96 al 2002; Bohrmann, & Zimmermann 2008; Sahu et al 2021). Several innexins, including Inx2, are
97 expressed in follicle cells and partially colocalize with or are juxtaposed to Inx4 (Bohrmann, &
98 Zimmermann 2008; Sahu et al 2021). Inx4 is required for germ cell survival before follicle formation,
99 and Inx2 is involved in the germline cyst encapsulation by follicle cells during follicle budding
100 (Gilboa et al 2003; Mukai et al 2011; Tazuke et al 2002). Inx2 and Inx4 are also required for
101 morphogenetic events during oogenesis. such as the stretching of anterior follicle cells and the
102 migration of border cells during stage 9 (Sahu et al 2021; Miao et al 2020). Moreover, Inx4 and
103 Inx2 form gap junctions in the testis where they are required at different steps of sperm
104 development (Tazuke et al 2002; Pesch et al 2022; Smendziuk et al 2015).
105 We found that Inx4/Inx2 gap junctions are required for female germline growth once follicles are
106 formed. Moreover, follicle cells specifically express genes involved in amino acid biology, and
107 proline import in follicle cells is necessary for germline growth. This germline growth control by
108 somatic follicle cells is linked to the formation of processing bodies (P-bodies) and can be partially
109 bypassed by the direct expression of a proline transporter in the germline. Moreover, gap junction

110 assembly is controlled by the InR/PI3K pathway, thus connecting growth coordination between
111 these two cell types with systemic growth control.
112

Results

Inx2 and Inx4 form gap junctions at the soma-germline interface that are required for germline growth

As gap junctions are required for oocyte growth in mammals, we asked whether they could play a similar role in *Drosophila* oogenesis (Gittens, & Kidder 2005; Simon et al 1997). Therefore, first, we characterized the gap junction composition and profile in somatic and germ cells, focusing on stages 1 to 8 when follicle development is globally limited to growth without major morphogenetic changes. As previously described (Tazuke et al 2002; Bohrmann, & Zimmermann 2008; Sahu et al 2021), we detected Inx2 and Inx4 forming plaques at the interface between germ and somatic cells. Inx2 also formed plaques on the lateral domain of follicle cells (Fig. 1B-E). Inx2 expression and plaque size tended to increase as follicles developed (Fig. S1). The cytoplasmic signal localization suggested that Inx2 and Inx4 were mainly expressed in the soma and germline, respectively. Accordingly, *Inx2* knock-down (*Inx2* RNAi) induction in somatic clones led to the cell-autonomous loss of Inx2 staining, whereas induction of *Inx4* knock-down (*Inx4* RNAi) in the germline led to the loss of Inx4 staining (Fig. 1F,G). Notably, we did not detect Inx4 at the contact of *Inx2* RNAi follicle cells, confirming published results (Fig. 1F''') (Sahu et al 2021). Similarly, when *Inx4* was knocked down in germline cysts, we did not detect Inx2 plaques at the germline contact, although Inx2 protein expression was increased in follicle cells (Fig. 1G'''). This observation could suggest a feedback mechanism between gap junction formation and Inx2 expression. Nonetheless, these data clearly established the presence of gap junction plaques composed of Inx4 in the germline and of Inx2 in follicle cells, and the Inx4-Inx2 interdependence for plaque assembly.

We then tested whether these gap junctions influenced germline growth by generating large *Inx2* mutant clones. In such conditions, we observed follicles that were smaller than the younger one at their anterior, a phenomenon never observed in the wild-type ovarioles. The quantification of the ratio between the volumes of the defective growth follicle and the follicle at its anterior confirmed these observations (Fig. 1H,I). We observed this phenotype with three different alleles, and only when all (or almost) epithelial cells of a follicle harboured the mutated *Inx2* while the anterior one was wild-type or contained a smaller percentage of mutant cells. A similar effect on the growth of the whole follicle was previously described for mutations affecting follicle cell growth (LaFever et al 2010; Maines et al 2004; Sun et al 2010; Vachias et al 2014b). However, follicles containing a mosaic of wild-type and *Inx2* mutant follicle cells grew normally and we did not observe any difference in cell size and in the proportion of cells in S phase (EDU-positive) between these populations, indicating that Inx2 did not influence somatic growth in a cell autonomous manner (Fig. 1J-K). This suggests that gap junctions are directly required for germline growth. We could not confirm this hypothesis using germline null *Inx4* mutant clones because in these mutants germline cyst development is blocked very early in the germanium (Tazuke et al 2002). Therefore,

150 we generated *Inx4* RNAi clones in the germline, directly detected by the absence of Inx4
151 expression (Fig. 1F). *Inx4* RNAi cysts were not larger than the younger wild-type follicle, indicating
152 defective germline growth (Fig. 1G). Altogether, these data indicate that Inx2 and Inx4 form
153 homomeric and heterotypic gap junctions between somatic and germ cells that are required for
154 germ cell growth.
155
156 **Genes implicated in amino acid metabolism are enriched in somatic follicular cells**
157 Gap junction requirement for germ cell growth supports a model in which metabolites diffuse from
158 follicle cells to germ cells. However, the direct identification of such metabolites is technically
159 challenging. We hypothesized that if follicle cells produce or import metabolites not present in the
160 germline, we might identify enzymes or transporters that are involved in this process and are
161 expressed only in follicle cells. To this aim, we performed translating ribosome affinity purification
162 (TRAP), an approach that allows identifying the tissue-specific translatome. We used
163 *nanos:Gal4VP16* and *trafficjam:Gal4* drivers to express a GFP-tagged ribosomal protein
164 (UASp:RPL10a-GFP) specifically in the germline and in somatic cells, respectively (Fig. 2A). Then,
165 we immunoprecipitated the GFP-tagged polysomes and isolated and sequenced the associated
166 mRNAs under translation. Our biological replicates were highly reproducible (Table S1). To extract
167 genes with a specific or strongly enriched somatic expression we used a fold-change of 5 between
168 soma and germline as cut-off that gave a list of 811 genes (Fig. 2B). We then selected genes
169 involved in small molecule metabolic processes, reducing the list to 52 genes. The whole
170 ecdysone synthesis pathway (six genes), which is exclusively active in follicle cells, was enriched
171 in follicle cells, thus validating our TRAP approach (Domanitskaya et al 2014). Moreover, six genes
172 encoding enzymes involved in amino acid biosynthesis were specifically expressed in follicle cells
173 (Fig. 2B). By analysing this GO class, we found that 29 enzymes were expressed in both cell types,
174 but none was germline-specific (Fig. 2C). Similarly, among the 60 amino acid transporters
175 encoded by the fly genome, 21 were expressed in both tissues, 12 were specifically expressed in
176 the soma, and none in the germline alone (Fig. 2B and D). These data indicated that among the
177 genes specifically expressed in follicle cells there is a strong bias for genes involved in amino acid
178 synthesis or import. Given the importance of these metabolites for growth, they are good
179 candidates to be transferred through gap junctions.
180
181 **Proline import in follicle cells is required for germline growth**

182 Then, we performed a reverse genetic screen by inducing the silencing (RNAi) of the genes
183 involved in amino acid synthesis or transport identified by TRAP in follicle cells and then looking
184 for ovary growth defects. For each amino acid many redundancies may occur between anabolic
185 pathways or transporters that may preclude the observation of clear phenotypes. However, the

186 knock-down of one of the 18 tested genes reproductively induced an ovary growth defect in
187 independent RNAi lines (Fig. 3B-C). This gene, *CG43693*, was uncharacterized in *Drosophila* but
188 showed a clear homology with SLC36 family transporters, and was especially close to mammalian
189 SLC36A1 and SLC36A that are mainly involved in proline transport (Boll et al 2002; Metzner et al
190 2006; Pillai, & Meredith 2011).

191 We confirmed by RNA-FISH that *CG43693* was specifically expressed in follicle cells (Fig 3D-E).
192 Moreover, we detected *CG43693* mRNA in all follicle cells and at all stages of oogenesis, and its
193 expression progressively increased with the stage (Fig. 3D). A role in importing amino acids from
194 the haemolymph would require a cell membrane localization, while some amino acid transporters
195 are specific to some intracellular vesicular compartments. Therefore, to determine CG43693
196 protein localization, we generated a GFP knock-in with the MiMIC system to insert in-frame an
197 EGFP-encoding exon (Venken et al 2011). This insertion was in the non-conserved N-terminal part
198 common to five of the seven described *CG43693* isoforms. Importantly, it tags isoforms RA and
199 RB that were expressed in follicle cells according to our TRAP mRNA sequence data. The line
200 C*G43693-GFP* was homozygous viable and fertile without visible phenotype, suggesting that the
201 insertion did not affect protein function. We observed a strong GFP signal in the whole cortex of
202 follicle cells that tended to increase throughout oogenesis, but no signal in the germline (Fig 3F-
203 G). Thus, both CG43693 tissue distribution and subcellular localization were in agreement with
204 the hypothesis that it is implicated in the import of metabolites, such as proline, to promote follicle
205 growth.
206 We then tested whether CG43693 was required for follicle growth. The Minos element insertion
207 (*CG43693*^{MI101960}) used for the GFP knock-in initially contains an exon with STOP codons in
208 different frames. As it is located in the protein N-terminus, it should induce null mutation of the
209 affected isoforms, which include the ones expressed in follicle cells. This line was homozygous
210 lethal. Replacing the STOP codon-containing exon with the GFP exon suppressed lethality,
211 indicating that it was due to the gene mutation. We generated mutant clones in the follicular
212 epithelium. Analysis of small clones that did not cover the whole epithelium did not show any
213 difference in cell size and proliferation, suggesting that follicle cell growth was not affected (Fig.
214 3J,K). Conversely, we observed follicles smaller (or of the same size) than the younger wild-type
215 one when the whole epithelium of a follicle was mutated (Fig. 3H,I). As this growth defect led to
216 tiny and round follicles, we called this gene *cochonnet (coch)* after the nickname of the small wood
217 ball used with larger metal boules for pétanque, a traditional game in the South of France.
218 Importantly, these experiments indicated that *coch* expression in somatic follicle cells was
219 required for germline growth.
220
221

222 **Genetic evidence of a metabolic transfer between soma and germline cells**
223 Our results support a model in which proline imported in follicle cells diffuses through gap
224 junctions to sustain germline growth. In this case, germline expression of *coch* should rescue
225 genetic conditions in which it is absent in somatic follicle cells. To test this hypothesis we
226 combined the UAS/Gal4 system with the QUAS/QF system (Potter et al 2010). We generated a
227 matTub:QF driver and a QUASp promoter, inspired by the UASp promoter, for proper expression
228 in the germline (Rørth 1998). The Q*UASp:GFP* transgene driven by matTub:QF was expressed in
229 the germline at all stages, starting slightly earlier than what described for matTub:Gal4Vp16,
230 indicating that both driver and QUASp promoter were functional (Fig. S2). Expression of the
231 *QUASp:coch* transgene in the germline with the same driver (*MatTub>coch*) had a slight negative
232 effect on ovary size (Fig. 4A-C,F). However, when it was combined with somatic knock-down of
233 *coch* (*tj>cochRNAi),* it rescued the effect of the latter on ovary size (Fig. 4A,D-F). These genetic
234 data demonstrated that the requirement of *coch* expression in follicular cells for germline growth
235 can be compensated by its germline expression, strongly arguing for a direct metabolic exchange
236 between these cell types.
237
238 **Blocking gap junctions or proline import induces processing bodies.**
239 Previous studies indicated that somatic growth impairment affects germ cell development
240 (LaFever et al 2010; Maines et al 2004; Sun et al 2010; Vachias et al 2014b). Moreover, the mRNA
241 binding protein Me31B, which is typically concentrated where the anterior-posterior axis
242 determinants localize in the oocyte, becomes enriched in large cytoplasmic structures in the
243 germline when somatic growth is impaired (Burn et al 2015; Shimada et al 2011). These
244 condensates are reminiscent of P-bodies and stress granules observed upon various stresses,
245 including amino acid deprivation (Riggs et al 2020). In follicles, their formation can be induced by
246 reducing protein availability in fly food and are more easily seen at stage 9 in Me31B-GFP-
247 expressing follicles (Shimada et al 2011) (Fig. 5A,B). Therefore, we set up a semi-automated
248 method for their quantification by measuring the fluorescence fraction found in condensates in
249 stage 9 nurse cells (Fig. 5C). P-body formation is associated with translation arrest usually induced
250 by inhibitory phosphorylation of the eukaryotic translation initiation factor 2 subunit alpha (eIF2α)
251 on serine 51 (S51) **(Riggs et al 2020)**. Overexpression in the germline of a transgene mimicking
252 this phosphorylated form (eIF2α-S51D), but not wild-type eIF2α, strongly induced P-body
253 formation, although we did not quantify them because these follicles never reached stage 9 (Fig.
254 5D,E). Importantly, eIF2α-S51D overexpression was sufficient to completely block germline
255 growth, suggesting a direct link between P-body formation and growth control (Fig. 5E). As P-
256 bodies potentially repress germline growth, we tested whether the absence of gap junctions
257 between germ cells and follicle cells or defective proline import in the follicle cells could induce
258 their formation. We knocked down *Inx2* and *coch* in follicle cells using *tj:Gal4* in the presence of

Me31B-GFP. Constitutive *Inx2* RNAi in the somatic lineage completely blocked oogenesis and precluded the observation of stages 8-9. Therefore, we added a constitutive *Gal80*^{ts} transgene to allow expression of the RNAi construct only during a short period of time at the permissive temperature (14 hours, at 30°C). *Coch* and *Inx2* knock-down strongly induced the formation of P-bodies, suggesting that the observed growth limitation was linked to their formation and the subsequent arrest of translation (Fig 5F-I).

Formation of P-bodies or stress granules following amino acid deprivation can occur independently or dependently of eIF2α S51 phosphorylation. In the first case, which is not the most frequently described, it is associated with the repression of the TOR pathway (Candena Sandoval et al 2021). However, induction of *Tor* RNAi in the germline does not induce P-body formation, excluding this possibility (Burn et al 2015). In the second case, eIF2α is phosphorylated by GCN2 that acts as an indirect sensor of amino acid availability. We generated null mutant alleles for *gcn2* that were homozygous viable, as similar alleles described during the course of this project (Kosakamoto et al 2022; Srivastava et al 2022; Kang et al 2017). Protein deprivation in *gcn2* transheterozygous females still led to P-body formation in the germ cells (Fig. S3A-E). Moreover, an indirect reporter of GCN2 activity and eIF2α–S51 phosphorylation showed no signal in the germline of wild-type flies, even after protein deprivation (Fig. S3F-G). Lastly, we tested more directly *gcn2* role in the germline when proline import in follicle cells is blocked (*tj>cochRNAi*). However, *gcn2* mutant germline clones did not increase the growth rate of wild-type and *coch* RNAi follicles (Fig. S3H,I). These results strongly argued against the implication of GCN2 as a germ cell growth repressor when proline availability is reduced.

Altogether these data indicate that although the two well-established pathways involved in amino acid sensing do not seem implicated, P-body formation is linked to germ cell growth control by gap junctions and proline import in follicle cells.

Gap junction assembly links intrinsic growth coordination and systemic control

Published data indicated that InR/PI3K pathway inhibition in follicle cells induces the formation of P-bodies in the germline (Burn et al 2015). This result was reproduced by silencing (RNAi) *akt*, an essential actor of this pathway, in follicle cells (Fig. 6A-C). Since somatic activity of the InR/PI3K pathway also strongly influences germline growth, we asked whether there was a link between the InR/PI3K pathway activity in follicle cells and their ability to transfer metabolites to the germline. Coch-GFP expression level and localization were similar in wild-type and in follicle cells with a PI3K gain of function or mutated for *akt,* suggesting no impact of this pathway on proline import in follicle cells (Fig. S4A,B). Conversely, in *akt* mutant cells, Inx2 was almost undetectable (Fig. 6D), whereas Inx2 expression was strongly increased in *Pten* mutant cells and plaques size was increased (Fig. 6E). These data indicated that Inx2 expression is sensitive to InR/PI3K pathway gain and loss of function. We also observed that *Inx2* mRNA level was strongly increased

296 in *Pten* mutant follicle cells, suggesting that the observed effects on protein level and plaque
297 assembly were due *Inx2* upregulation (Fig. 6F). These observations supported a model in which
298 the non-cell autonomous effect of the InR/PI3K pathway from somatic cells to germ cells is
299 mediated by gap junctions. To test this hypothesis, we performed an epistasis experiment. As
300 previously described (Vachias et al 2014a), large *Pten* mutant clones in the follicular epithelium
301 accelerated germline growth in a non-cell autonomous manner (Fig. 6G). This effect was
302 abrogated upon *Inx2* RNAi induction in *Pten* mutant cells (Fig. 6H). Thus, gap junctions are
303 required for germline growth control via InR/PI3K activity in the follicular epithelium. Altogether,
304 our data link the systemic control of somatic cells to the growth coordination between somatic
305 and germline cells via the modulation of gap junction assembly.
306
307

Discussion

In this article we show how gap junctions participate in cell growth control by allowing a metabolic flow between cells. This is illustrated by the identification of a proline transporter specifically expressed in follicle cells and required for germline cell growth. Importantly, its expression in the germline can partially bypass its silencing in the soma, providing evidence for a functional metabolic exchange between these cell types.

Inx2 and Inx4 have various functions during *Drosophila* oogenesis (Mukai et al 2011; Sahu et al 2021; Tazuke et al 2002; Miao et al 2020). However, our data showing their involvement in germ cell growth can be more easily compared with gap junction role in mammal follicles where Cx37 is expressed in the oocyte and Cx43 in follicle cells (Gittens, & Kidder 2005; Simon et al 1997). This indicates that gap junction requirement for oocyte growth is a conserved feature throughout evolution. Gap junctions are present in most animal tissues and can directly connect different cell types, for instance, neurons and glial cells. Therefore, their involvement in growth control might be more general. We found that Inx2 expression and the subsequent formation of plaques were strongly regulated by the InR/PI3K pathway in a cell autonomous manner. This indicates that gap junctions are a permissive prerequisite for germline growth, and it also provides an effective mechanism to link metabolic flow with growth systemic signals and coordinate the growth of the two connected cell populations.

Our results also established that Coch (CG43693), a putative proline transporter of the SLC36A family, must be expressed in somatic cells for germline growth. Proline import is important for cell growth in different contexts, including in cancer (Geng et al 2021; Newton et al 2020). It is usually proposed that TOR signalling links proline availability and cell growth control (Shang et al 2017; Yoshida et al 2019; Zhao et al 2019). However, this pathway is unlikely implicated in the mechanism described here. Indeed, first, when germline growth is blocked due to alteration of somatic cell growth upon loss of *akt*, which also regulates gap junction assembly, the TOR pathway is still active in the germline (Vachias et al 2014b). Moreover, overactivation of the TOR pathway in the germline in such conditions does not suppress growth inhibition. Finally, TOR inhibition in the *Drosophila* female germline does not induce P-body formation (Burn et al 2015). Therefore, we tested the involvement of the other well-described amino acid sensing pathway that relies on GCN2. Our results also excluded this mechanism to explain P-body formation and growth inhibition in the absence of proline import in somatic cells or of gap junctions. Therefore, more studies are needed to determine the precise mechanism underlying germline growth control. Nevertheless, several arguments suggest that proline import might just be the tip of the iceberg of the metabolic cooperativity between follicle cells and germ cells. *Inx2* mutant clones have a stronger impact on germline growth than *coch* mutant clones, suggesting that other metabolites from follicle cells also may promote germline growth. Accordingly, our translatome analysis showed that different genes involved in amino acid synthesis or import were specifically

346 expressed in follicle cells, but none in germ cells. The absence of phenotype when these genes
347 were knocked down, except *coch*, could be explained by multiple potential levels of redundancy
348 among synthesis pathways, transporters, and synthesis and import. Nonetheless, detailed
349 analysis of the genes overexpressed in follicle cells compared with germ cells suggest that other
350 amino acids (e.g. tryptophane, valine, tyrosine) could flow from the soma to the germline.
351 Moreover, in the mouse, the alanine transporter SLC38A3 is strongly enriched in granulosa cells
352 that are required for efficient alanine import in the oocyte (Eppig et al 2005). Thus, altogether these
353 data suggest that gap junction-dependent amino acid flow is not restricted to proline. Moreover,
354 glucose intake and pyruvate production are more efficient in granulosa cells, suggesting that
355 follicle cells could provide energetic molecules to the oocyte (Sugiura et al 2005). In line with this
356 observation in mammals, TRAP data indicated that transporter for trehalose (tret1-1), the
357 circulating sugar in insects, was expressed in somatic cells and not in the germline, whereas
358 germline development is highly dependent on sugar and the pentose phosphate pathway
359 (Carvalho-Santos et al 2020). Importantly, it has been recently shown that glucose availability and
360 ATP production regulate stress granules in yeast, suggesting that a link between growth control
361 and energy molecule disposal could also exist during germline development (Cereghetti et al
362 2021). Sperm development also relies on a specific metabolic programme suggesting that gap
363 junction-dependent metabolic cooperativity could participate in spermatogenesis (Hudry et al
364 2019). Thus, a contribution of energetic metabolism in the soma-germline cooperativity via gap
365 junctions will be an interesting avenue for future investigations.
366 One might ask what is the evolutive advantage of this metabolic cooperativity compared with
367 direct import or synthesis in the germline. Two main hypotheses could be proposed. First, female
368 germ cells undergo massive growth and there is a non-linear relation between volume and cell
369 surface increases. Consequently, surface exchange with the extracellular medium might not allow
370 sufficient metabolic import and may require the support of follicle cells. This hypothesis was
371 proposed to explain gap junction requirement for mammal oocyte growth (Su et al 2009).
372 However, in this case, both tissues should be able to import the required metabolites and our data
373 does not support such a model because follicle cells expressed a whole set of anabolic enzymes
374 and transporters that were not expressed in the germline. Alternatively, such a mechanism may
375 provide a protective effect for the germline. It is well established that the cell metabolic activity
376 can induce stress, with for instance, the production of reactive oxygen species (ROS). However,
377 the germline must be protected, especially its DNA content that is transmitted to the embryo. A
378 recent study demonstrated that mammalian oocytes block ROS production by suppressing
379 mitochondrial complex I (Rodríguez-Nuevo et al 2022). Thus, a gap junction-mediated metabolic
380 exchange might allow externalizing the stress-generating metabolic activity to follicle cells that
381 will anyway die few days later. Notably, *coch* expression in germ cells had a slight but significant
382 negative impact on ovary size, suggesting that its presence in germ cells is detrimental for follicle

383 development. Although, the exact reason for this deleterious effect is unknown, this observation
384 fits with a model in which externalization of metabolic import and activity could facilitate proper
385 oocyte development. However, Coch is a transporter, and not an enzyme, and thus, the protective
386 effect might not be directly due to proline exclusion, but to one of the many possible downstream
387 metabolic activities (Patriarca et al 2021).
388 Altogether, our data establish that metabolic flow through gap junctions is essential for cell growth
389 and that gap junction assembly can be modulated to adjust cell growth rate. Moreover, it shows
390 that amino acids, and potentially other metabolites, are important actors in this mechanism ending
391 with the formation of P-bodies, opening a large field for investigation to obtain a comprehensive
392 view of this metabolic cooperativity.
393

394 **Methods**

395

396 **Fly genetics and handling**

397 All fly stocks used are detailed in Table S2. The final genotypes, temperature and heat-shock
398 conditions are in Table S3. *gcn2* null alleles were generated by inducing indel mutations using an
399 available gRNA line. Alleles are described in Table S2. Unless specified, flies were kept on a corn
400 meal-based medium with 80 g/L fresh yeast. Protein starvation was performed on grape juice agar
401 plate. Coch-EGFP was obtained by inserting the EGFP-FlAsH-StrepII-TEV-3xFlag cassette in the
402 Minos element insertion MI01960, as previously described (Venken et al 2011).

403 **TRAP experiments**

404 Ovaries of 100 females of each genotype (tj>RPL10-GFP or Nos>RPL10-GFP) were dissected on
405 ice. Then, TRAP was performed as described in Bertin et al, 2015. Briefly, after homogenization,
406 ovary extracts were preabsorbed with magnetic beads. Immunoprecipitation was performed with
407 anti-GFP antibodies already coupled with magnetic beads before mRNA extraction. Tissue
408 specificity and enrichment of the extracted mRNAs were checked by RT-qPCR with *GFP*
409 (enrichment), *traffic-jam* (soma specific), *Ago3* and *Aubergine* (germline specific) primers. mRNA
410 libraries were made with the Nugen Ovation 1-16 droso Universal RNA-seq kit according to the
411 manufacturer's instructions. Sequencing was performed by Fasteris. Data were deposited on GEO
412 (GSE230452) and described in Table S1.

413 **Molecular cloning and transgenesis**

414 The *QF* sequence was amplified from the pAttB-QF-sv40 vector and cloned in the vector that
415 contains the alpha4-tubulin promoter (mat-tub). The pQUASp vector was constructed from
416 pUAST in which the promoter was replaced by QUAS sites and the minimal P-element promoter
417 was amplified from the pUASp vector. Then, this vector was used to clone *EGFP* or *coch* coding
418 sequence and P-element insertions were generated. *eIF2α* and *eIF2α-S51D* coding sequences
419 were cloned in the pUASz vector, and transgenes were inserted at the AttP40 landing site.

420 **Immunostaining, FISH, EDU incorporation, imaging and quantitative analyses**

421 Resources and reagents are listed in Table S1. Immunostaining was performed as described in
422 Vachias et al, 2013. Stellaris SM-FISH oligo-probes against *Inx2* and *CG43693/coch* mRNAs were
423 produced by Biosearch Technologies. FISH was performed according to the manufacturer's
424 instruction. Images were acquired on a Zeiss LSM800 confocal microscope or a Zeiss Cell
425 observer spinning disc microscope. P-bodies were quantified using a homemade macro initially
426 designed to quantify basement membrane fibrils (Cerqueira Campos et al 2020). Quantifications
427 were done on 5 μm z-stack projections of spinning-disc images acquired with a x20 lens. After
428 manual selection of a ROI corresponding to nurse cells, P-bodies were detected by keeping
429 objects with a minimal size of 5 adjacent pixels and a minimal fluorescence intensity of x1.75 of
430 the mean intensity. Then, the total fluorescence contained in these P-bodies was quantified and

431 reported as a fraction of the total fluorescence of the ROI. For EDU incorporation, ovaries were
432 incubated with 10μM EDU in complemented Schneider medium for 15 minutes. After fixation,
433 staining was performed according to the manufacturer's instructions (Kit EDU C10638, Thermo
434 Fisher). Mutant-control follicle volume ratios were calculated after estimating the follicle volume
435 by multiplying their length by their width to the square. Mutant and control follicles in position 2
436 or 3 of the ovariole starting from the anterior were analysed. Cell size was automatically
437 determined after cell segmentation using Tissue Analyzer (Aigouy et al 2016). Statistical analyses
438 were performed with Prism. For all experiments, the minimum sample size is indicated in the figure
439 legends. For each experiment, multiple females were dissected. Randomization or blinding was
440 not performed. The sample normality was calculated using the D'Agostino and Pearson normality
441 test. The unpaired *t*-test was used to compare samples with normal distribution (or one-way
442 ANOVA for multiple comparisons), and the unpaired Mann–Whitney test for samples without
443 normal distribution. Figures were prepared using ScientiFig (Aigouy, & Mirouse 2013).
444
445

Acknowledgements

We are grateful to G. Junion, P Phelan, G Tanentzapf, H.D. Ryoo for sharing antibodies or fly stocks. This research was financed by the French government IDEX-ISITE initiative 16-IDEX-0001 (CAP 20-25). We also thank the CLIC facility (Clermont Imagerie Confocale).

452 **References**

453 Aigouy, B. & Mirouse, V., 2013, ScientiFig: a tool to build publication-ready scientific figures,
454 *Nature methods*, 10(11), p. 1048.
455 Aigouy, B., Umetsu, D. & Eaton, S., 2016, Segmentation and Quantitative Analysis of Epithelial
456 Tissues, *Methods in molecular biology (Clifton, N.J.)*, 1478, pp. 227-39.
457 Bauer, R., Löer, B., Ostrowski, K., Martini, J., Weimbs, A., Lechner, H. & Hoch, M., 2005,
458 Intercellular communication: the Drosophila innexin multiprotein family of gap junction proteins,
459 *Chemistry & biology*, 12(5).
460 Bohrmann, J. & Zimmermann, J., 2008, Gap junctions in the ovary of Drosophila melanogaster:
461 localization of innexins 1, 2, 3 and 4 and evidence for intercellular communication via innexin-2
462 containing channels, *BMC developmental biology*, 8, p. 111.
463 Boll, M., Foltz, M., Rubio-Aliaga, I., Kottra, G. & Daniel, H., 2002, Functional characterization of
464 two novel mammalian electrogenic proton-dependent amino acid cotransporters, *The Journal of*
465 *biological chemistry*, 277(25).
466 Borreguero-Muñoz, N., Fletcher, G.C., Aguilar-Aragon, M., Elbediwy, A., Vincent-Mistiaen, Z.I. &
467 Thompson, B.J., 2019, The Hippo pathway integrates PI3K-Akt signals with mechanical and
468 polarity cues to control tissue growth, *PLoS biology*, 17(10), p. e3000509.
469 Burn, K.M., Shimada, Y., Ayers, K., Vemuganti, S., Lu, F., Hudson, A.M. & Cooley, L., 2015,
470 Somatic insulin signaling regulates a germline starvation response in Drosophila egg chambers,
471 *Developmental biology*, 398(2).
472 Cadena Sandoval, M., Heberle, A.M., Rehbein, U., Barile, C., JM, R.P. & Thedieck, K., 2021,
473 mTORC1 Crosstalk With Stress Granules in Aging and Age-Related Diseases, *Frontiers in aging*,
474 2.(M
475 Carvalho-Santos, Z., Cardoso-Figueiredo, R., Elias, A.P., Tastekin, I., Baltazar, C. & Ribeiro, C.,
476 2020, Cellular metabolic reprogramming controls sugar appetite in Drosophila, *Nature*
477 *metabolism*, 2(9).
478 Cereghetti, G., Wilson-Zbinden, C., Kissling, V.M., Diether, M., Arm, A., Yoo, H., Piazza, I., Saad,
479 S., Picotti, P., Drummond, D.A., Sauer, U., Dechant, R. & Peter, M., 2021, Reversible amyloids of
480 pyruvate kinase couple cell metabolism and stress granule disassembly, *Nature cell biology*,
481 23(10).
482 Cerqueira Campos, F., Dennis, C., Alégot, H., Fritsch, C., Isabella, A., Pouchin, P., Bardot, O.,
483 Horne-Badovinac, S. & Mirouse, V., 2020, Oriented basement membrane fibrils provide a
484 memory for F-actin planar polarization via the Dystrophin-Dystroglycan complex during tissue
485 elongation, *Development*, 147(7).
486 Chen, D.Y., Crest, J., Streichan, S.J. & Bilder, D., 2019, Extracellular matrix stiffness cues
487 junctional remodeling for 3D tissue elongation, *Nature communications*, 10(1).
488 Church, S.H., Donoughe, S., BAS, D.M. & Extavour, C.G., 2019, Insect egg size and shape
489 evolve with ecology but not developmental rate, *Nature*, 571(7763).
490 Doherty, C.A., Amargant, F., Shvartsman, S.Y., Duncan, F.E. & Gavis, E.R., 2022, Bidirectional
491 communication in oogenesis: a dynamic conversation in mice and Drosophila, *Trends in cell*
492 *biology*, 32(4).
493 Doherty, C.A., Diegmiller, R., Kapasiawala, M., Gavis, E.R. & Shvartsman, S.Y., 2021, Coupled
494 oscillators coordinate collective germline growth, *Developmental cell*, 56(6).
495 Domanitskaya, E., Anllo, L. & Schüpbach, T., 2014, Phantom, a cytochrome P450 enzyme
496 essential for ecdysone biosynthesis, plays a critical role in the control of border cell migration in
497 Drosophila, *Developmental biology*, 386(2).
498 Drummond-Barbosa, D. & Spradling, A.C., 2001, Stem cells and their progeny respond to
499 nutritional changes during Drosophila oogenesis, *Developmental biology*, 231(1), pp. 265-78.
500 Elias, L.A., Wang, D.D. & Kriegstein, A.R., 2007, Gap junction adhesion is necessary for radial
501 migration in the neocortex, *Nature*, 448(7156).
502 Eppig, J.J., Pendola, F.L., Wigglesworth, K. & Pendola, J.K., 2005, Mouse oocytes regulate
503 metabolic cooperativity between granulosa cells and oocytes: amino acid transport, *Biology of*
504 *reproduction*, 73(2).
505 Evans, W.H., 2015, Cell communication across gap junctions: a historical perspective and
506 current developments, *Biochemical Society transactions*, 43(3).

Geng, P., Qin, W. & Xu, G., 2021, Proline metabolism in cancer, *Amino acids*, 53(12).
Gilboa, L., Forbes, A., Tazuke, S.I., Fuller, M.T. & Lehmann, R., 2003, Germ line stem cell differentiation in Drosophila requires gap junctions and proceeds via an intermediate state, *Development*, 130(26).
Gittens, J.E. & Kidder, G.M., 2005, Differential contributions of connexin37 and connexin43 to oogenesis revealed in chimeric reaggregated mouse ovaries, *Journal of cell science*, 118(Pt 21).
Hudry, B., E, D.G., Mineo, A., Gaspar, P., Hadjieconomou, D., Studd, C., Mokochinski, J.B., Kramer, H.B., Plaçais, P.Y., Preat, T. & Miguel-Aliaga, I., 2019, Sex Differences in Intestinal Carbohydrate Metabolism Promote Food Intake and Sperm Maturation, *Cell*, 178(4).
Kang, M.J., Vasudevan, D., Kang, K., Kim, K., Park, J.E., Zhang, N., Zeng, X., Neubert, T.A., Marr, M.T. & Ryoo, H.D., 2017, 4E-BP is a target of the GCN2-ATF4 pathway during Drosophila development and aging, *The Journal of cell biology*, 216(1).
Kosakamoto, H., Okamoto, N., Aikawa, H., Sugiura, Y., Suematsu, M., Niwa, R., Miura, M. & Obata, F., 2022, Sensing of the non-essential amino acid tyrosine governs the response to protein restriction in Drosophila, *Nature metabolism*, 4(7).
LaFever, L., Feoktistov, A., Hsu, H.J. & Drummond-Barbosa, D., 2010, Specific roles of Target of rapamycin in the control of stem cells and their progeny in the Drosophila ovary, *Development*, 137(13), pp. 2117-26.
Maines, J.Z., Stevens, L.M., Tong, X. & Stein, D., 2004, Drosophila dMyc is required for ovary cell growth and endoreplication, *Development*, 131(4), pp. 775-86.
Metzner, L., Neubert, K. & Brandsch, M., 2006, Substrate specificity of the amino acid transporter PAT1, *Amino acids*, 31(2).
Miao, G., Godt, D. & Montell, D.J., 2020, Integration of Migratory Cells into a New Site In Vivo Requires Channel-Independent Functions of Innexins on Microtubules, *Developmental cell*, 54(4).
Michel, D., Arsanto, J.P., Massey-Harroche, D., Béclin, C., Wijnholds, J. & Le Bivic, A., 2005, PATJ connects and stabilizes apical and lateral components of tight junctions in human intestinal cells, *Journal of cell science*, 118(Pt 17), pp. 4049-57.
Mukai, M., Kato, H., Hira, S., Nakamura, K., Kita, H. & Kobayashi, S., 2011, Innexin2 gap junctions in somatic support cells are required for cyst formation and for egg chamber formation in Drosophila, *Mechanisms of development*, 128(7-10).
Newton, H., Wang, Y.F., Camplese, L., Mokochinski, J.B., Kramer, H.B., AEX, B., Fets, L. & Hirabayashi, S., 2020, Systemic muscle wasting and coordinated tumour response drive tumourigenesis, *Nature communications*, 11(1).
Oshima, A., Tani, K. & Fujiyoshi, Y., 2016, Atomic structure of the innexin-6 gap junction channel determined by cryo-EM, *Nature communications*, 7.
Patriarca, E.J., Cermola, F., D'Aniello, C., Fico, A., Guardiola, O., D, D.C. & Minchiotti, G., 2021, The Multifaceted Roles of Proline in Cell Behavior, *Frontiers in cell and developmental biology*, 9.
Pesch, Y.Y., Dang, V., Fairchild, M.J., Islam, F., Camp, D., Kaur, P., Smendziuk, C.M., Messenberg, A., Carr, R., McFarlane, C.R., Musso, P.Y., F, V.P. & Tanentzapf, G., 2022, Gap junctions mediate discrete regulatory steps during fly spermatogenesis, *PLoS genetics*, 18(9).
Petkova, M.D., Little, S.C., Liu, F. & Gregor, T., 2014, Maternal origins of developmental reproducibility, *Current biology : CB*, 24(11), pp. 1283-8.
Pillai, S.M. & Meredith, D., 2011, SLC36A4 (hPAT4) is a high affinity amino acid transporter when expressed in Xenopus laevis oocytes, *The Journal of biological chemistry*, 286(4).
Potter, C.J., Tasic, B., Russler, E.V., Liang, L. & Luo, L., 2010, The Q system: a repressible binary system for transgene expression, lineage tracing, and mosaic analysis, *Cell*, 141(3).
Riggs, C.L., Kedersha, N., Ivanov, P. & Anderson, P., 2020, Mammalian stress granules and P bodies at a glance, *Journal of cell science*, 133(16).
Rodríguez-Nuevo, A., Torres-Sanchez, A., Duran, J.M., De Guirior, C., Martínez-Zamora, M.A. & Böke, E., 2022, Oocytes maintain ROS-free mitochondrial metabolism by suppressing complex I, *Nature*, 607(7920), pp. 756-61.
Rørth, P., 1998, Gal4 in the Drosophila female germline, *Mechanisms of development*, 78(1-2).

560 Sahu, A., Karmakar, S., Halder, S., Ghosh, G., Acharjee, S., Dasgupta, P., Ghosh, R.,
561 Deshpande, G. & Prasad, M., 2021, Germline soma communication mediated by gap junction
562 proteins regulates epithelial morphogenesis, *PLoS genetics*, 17(8).
563 Shang, P., Valapala, M., Grebe, R., Hose, S., Ghosh, S., Bhutto, I.A., Handa, J.T., Lutty, G.A., Lu,
564 L., Wan, J., Qian, J., Sergeev, Y., Puertollano, R., Zigler, J.S., Xu, G.T. & Sinha, D., 2017, The
565 amino acid transporter SLC36A4 regulates the amino acid pool in retinal pigmented epithelial
566 cells and mediates the mechanistic target of rapamycin, complex 1 signaling, *Aging cell*, 16(2).
567 Shimada, Y., Burn, K.M., Niwa, R. & Cooley, L., 2011, Reversible response of protein localization
568 and microtubule organization to nutrient stress during Drosophila early oogenesis,
569 *Developmental biology*, 355(2).
570 Simon, A.M., Goodenough, D.A., Li, E. & Paul, D.L., 1997, Female infertility in mice lacking
571 connexin 37, *Nature*, 385(6616).
572 Skerrett, I.M. & Williams, J.B., 2017, A structural and functional comparison of gap junction
573 channels composed of connexins and innexins, *Developmental neurobiology*, 77(5).
574 Smendziuk, C.M., Messenberg, A., Vogl, A.W. & Tanentzapf, G., 2015, Bi-directional gap
575 junction-mediated soma-germline communication is essential for spermatogenesis,
576 *Development*, 142(15).
577 Spradling, A.C., Bate, M. & Arias, A.M., 1993, The development of Drosophila melanogaster, *The*
578 *Development of Drosophila Melanogaster*, 1, pp. 1-70.
579 Srivastava, A., Lu, J., Gadalla, D.S., Hendrich, O., Grönke, S. & Partridge, L., 2022, The Role of
580 GCN2 Kinase in Mediating the Effects of Amino Acids on Longevity and Feeding Behaviour in
581 Drosophila, *Frontiers in aging*, 3.
582 Su, Y.Q., Sugiura, K. & Eppig, J.J., 2009, Mouse oocyte control of granulosa cell development
583 and function: paracrine regulation of cumulus cell metabolism, *Seminars in reproductive*
584 *medicine*, 27(1), pp. 32-42.
585 Sugiura, K., Pendola, F.L. & Eppig, J.J., 2005, Oocyte control of metabolic cooperativity
586 between oocytes and companion granulosa cells: energy metabolism, *Developmental biology*,
587 279(1).
588 Sun, P., Quan, Z., Zhang, B., Wu, T. & Xi, R., 2010, TSC1/2 tumour suppressor complex
589 maintains Drosophila germline stem cells by preventing differentiation, *Developmen)*, 137(15),
590 pp. 2461-9.
591 Tazuke, S.I., Schulz, C., Gilboa, L., Fogarty, M., Mahowald, A.P., Guichet, A., Ephrussi, A.,
592 Wood, C.G., Lehmann, R. & Fuller, M.T., 2002, A germline-specific gap junction protein required
593 for survival of differentiating early germ cells, *Development*, 129(10).
594 Vachias, C., Fritsch, C., Pouchin, P., Bardot, O. & Mirouse, V., 2014a, Tight coordination of
595 growth and differentiation between germline and soma provides robustness for drosophila egg
596 development, *Cell reports*, 9(2), pp. 531-41.
597 Vachias, C., Fritsch, C., Pouchin, P., Bardot, O. & Mirouse, V., 2014b, Tight coordination of
598 growth and differentiation between germline and soma provides robustness for drosophila egg
599 development, *Cell reports*, 9(2), pp. 531-41.
600 Venken, K.J., Schulze, K.L., Haelterman, N.A., Pan, H., He, Y., Evans-Holm, M., Carlson, J.W.,
601 Levis, R.W., Spradling, A.C., Hoskins, R.A. & Bellen, H.J., 2011, MiMIC: a highly versatile
602 transposon insertion resource for engineering Drosophila melanogaster genes, *Nature methods*,
603 8(9), pp. 737-43.
604 Wang, Y. & Riechmann, V., 2007, The role of the actomyosin cytoskeleton in coordination of
605 tissue growth during Drosophila oogenesis, *Current biology : CB*, 17(15), pp. 1349-55.
606 Yoshida, A., Bu, Y., Qie, S., Wrangle, J., Camp, E.R., Hazard, E.S., Hardiman, G., R, D.L.,
607 Knudsen, K.E. & Diehl, J.A., 2019, SLC36A1-mTORC1 signaling drives acquired resistance to
608 CDK4/6 inhibitors, *Science advances*, 5(9).
609 Zhao, L., Zhang, X., Ji, X., Jin, Y. & Liu, W., 2019, The amino acid transporter PAT1 regulates
610 mTORC1 in a nutrient-sensitive manner that requires its transport activity, *Cellular signalling*, 53.
611
612

613 **Figure legends**

614

615 **Figure 1: Soma-germline gap junctions are required for germline growth**

616 A) Scheme of an ovariole, oriented from the anterior (A) to the posterior (P) end, as all the
617 subsequent images. The ovariole starts with the germarium from which young follicles bud before
618 undergoing massive growth until the formation of an egg at the posterior end. In each follicle,
619 somatic follicle cells (in purple) surround a germline cyst with the nurse cells (pink) and the oocyte
620 (in blue). B) Sagittal view and C) Maximum intensity projection images of a stage 7 follicle after
621 immunostaining for Inx2 (green in B and C, white in B' and C') and Inx4 (magenta in B and C, white
622 in B'' and C''). D) and E) Higher magnification of the insets in B and C to illustrate the formation of
623 plaques at the germline-soma interface. F) Immunostaining for Inx2 (green in F and F', white in
624 F''') and Inx4 (magenta in F', white in F'') in a follicle containing a *Inx2* RNAi-expressing clone in
625 follicle cells marked by GFP expression (white in F). G) Immunostaining for Inx2 (green in G, white
626 in G'' and G''') and Inx4 (magenta in G, white in G') in follicles containing *Inx4* RNAi-expressing
627 germline clones visualized by Inx4 absence. Note the absence of Inx2 plaques at germline
628 contacts at higher magnification (G''') and the growth defect of *Inx4* RNAi follicles compared with
629 the wild-type younger follicle (G). H) Somatic $Inx2^{A}$ mutant clones, marked by the absence of RFP
630 expression, induce a germline growth defect when they cover the whole epithelium. I)
631 Quantification of the ratio between the volume of the follicle showing a growth defect (fully covered
632 by *Inx2* mutant cells) and the volume of the n-1 follicle of the same ovariole (n= 10 control and 7
633 *Inx2* mutant follicles). J-K) quantification of J) cell surface incorporation and K) EDU-positive cells
634 in small mutant *Inx2* clones compared with the surrounding wild-type cells (n= 20, 20 clones or
635 groups of wild-type cells for J and K). For all graphs, data are the mean ± SD. ***p <0.01. Scale
636 bars: 20 μm.

637

638 **Figure 2: TRAP analysis identifies soma-specific expression of amino acid metabolism and**
639 **transport genes**

640 A) Representative images of follicles expressing RPL10a-GFP in the soma (driven by tj:Gal4) or
641 the germline (driven by nos:Gal4p16). After polysome immunoprecipitation (IP), mRNAs were
642 sequenced. B) The expression of 811 genes was significantly enriched in somatic cells compared
643 with germline cells (fold change >5, p-value <0.05). After filtering for genes involved in small
644 molecule metabolism or transport, genes related to amino acid biology were identified. C)
645 Distribution (soma and/or germline) of genes encoding proteins implicated in amino acid
646 biosynthesis or transport according to their expression profile. No gene was enriched exclusively
647 in the germline.

648

649 **Figure 3: Proline import in follicle cells promotes germline growth**

650 A-B) Representative images of ovaries in A) control and B) after *CG43693* knock-down by RNAi
651 in somatic cells. C) Ovary size (surface) quantification in control and after *CG43693* somatic
652 knock-down using two RNAi lines. D-E) In situ hybridization analysis of *CG43693* expression in D)
653 a whole ovariole and in E) stage 4 and 7 follicles. F) Expression of endogenous CG43693 protein
654 tagged with GFP from germarium to stage 8. G) Higher magnification of follicle cells showing
655 CG43693-GFP localization in the cell cortex. H) *CG43693/cochonnet (coch)* mutant clones
656 marked by the absence of RFP. When all follicle cells are mutated, follicle growth is affected. I)
657 Quantification of the ratio between the volume of follicle with a growth defect and fully covered by
658 mutant cells and the n-1 follicle in the same ovariole (n= 10 control and 6 *coch* mutant follicles).
659 J-K) quantification of J) EDU-positive cells and K) cell surface in small *coch* mutant clones
660 compared with the surrounding wild-type cells (n=12 control and 12 mutant clones or groups of
661 wild-type cells). For all graphs, data are the mean ± SD. **p <0.01, ***p <0.001. Scale bars: 50 μm
662 in D,E,F,H and 20 μm in G.
663
664 **<u>Figure 4:</u> Ectopic proline import in the germline compensates its absence in the soma**
665 A) scheme representating *coch* expression in green in the different genotypes used on this figure.
666 B-E) Representative images of a full ovary from B) a control female, C) a *MatTub> coch* female D)
667 a *tj > coch RNAi* female, and E) a *tj > coch RNAi*, *MatTub> coch* female. C) Quantification of ovary
668 size (surface) in the indicated genotypes (n = 14, 10, 19, and 27 ovaries). For all graphs, data are
669 the mean ± SD., ***p <0.001, ****p <0.0001. Scale bars: 50 μm.
670
671 **<u>Figure 5:</u> Defective gap junctions or proline import induces P-body formation**
672 A-B) Endogenous GFP-tagged Me31B protein expression in stage 9 follicles in A) well fed
673 conditions or B) after 15 hours of protein starvation. C) P-body quantification in normal and starved
674 conditions. D-E) Me31B-GFP expression in ovarioles germline that overexpresses D) wild-type
675 eIF2α or E) or eIF2α-S51D (inhibitory phosphorylation). F and H) Representative images of Me31B-
676 GFP expression in stage 9 follicles after RNAi-based knock-down in somatic cells of F) *Inx2* or H)
677 *coch*. G and I) P-body quantification in follicles after RNAi-based knock-down in somatic cells of
678 G) *Inx2* and I) *coch.* For all graphs, data are the mean ± SD, ****p <0.0001. Scale bars: 50 μm.
679
680 **<u>Figure 6:</u> Gap junction are controlled by the InR/PI3K pathway**
681 A,B) Representative images of Me31B-BFP expression in stage 9 follicles from A) a control female
682 and B) a *tj:Gal4, Tub:Gal80^{ts} > akt RNAi* female. C) P-body quantification (fluorescence intensity)
683 in the indicated genotypes (n = 8 and 9 follicles). Data are the mean ± SD. ****p <0.0001. D) Inx2
684 expression in an *akt^{q}* mutant clone (marked by the absence of GFP expression). E-F) Inx2 protein
685 (E) and *Inx2* mRNA expression by FISH (F) in a *Pten^{dj189}* mutant clone marked by the absence of
686 RFP expression. G) Large MARCM *Pten^{dj189}* mutant clone marked by the absence of GFP

687 expression showing faster follicle growth. H) Large MARCM *Pten*^{dj189} mutant clone in which faster
688 follicle growth was abolished after expression of an RNAi against *Inx2*. Scale bars: 50 μm in A, B,
689 G, H and 20 μm in D,E,F.
690
691

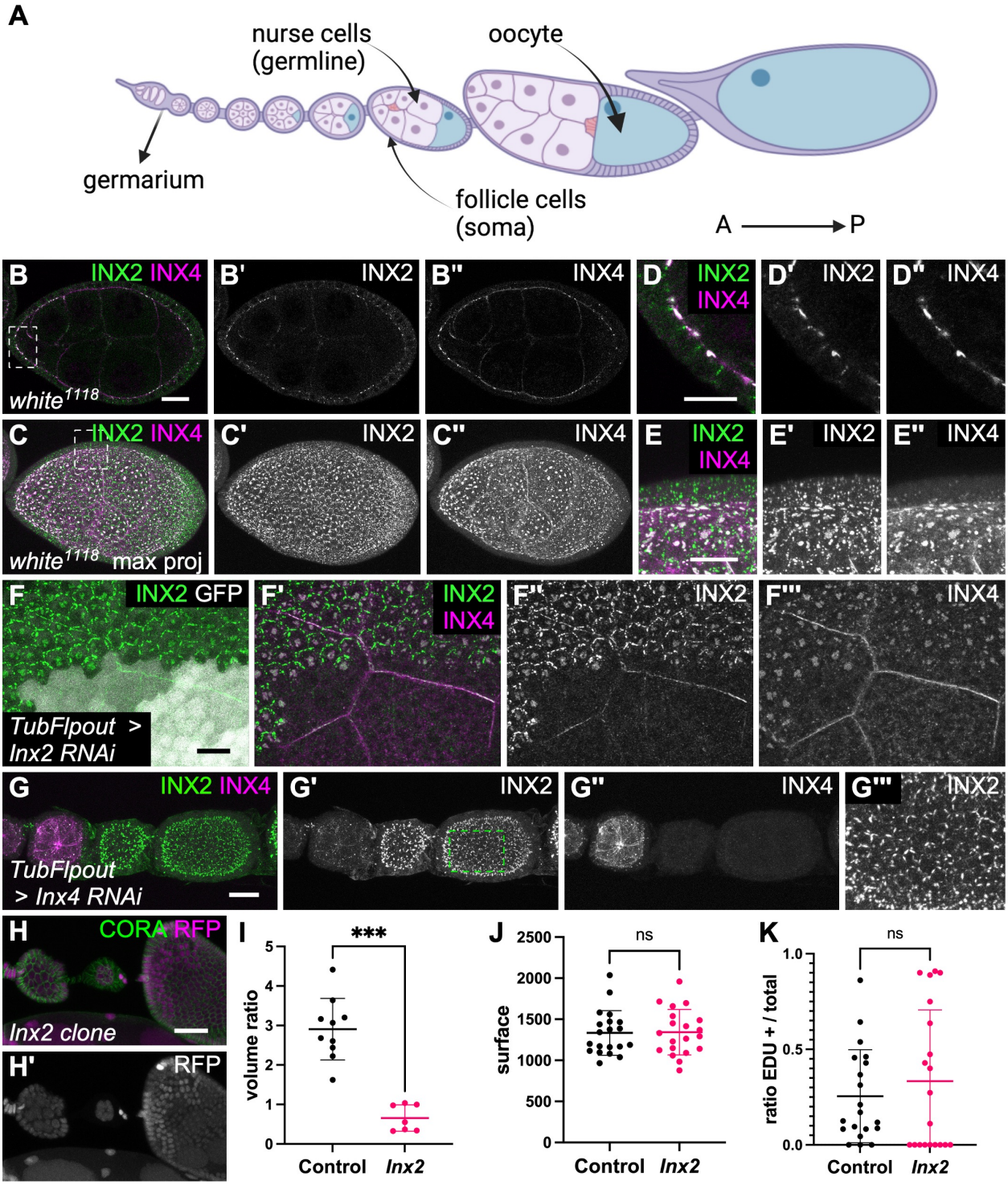
A
nurse cells
(germline)
oocyte
germarium
follicle cells
(soma)
A
P
B
INX2 INX4
white1118
B'
INX2
B''
INX4
D
INX2
INX4
D'
INX2
D''
INX4
C
INX2 INX4
white1118
max proj
C'
INX2
C''
INX4
E
INX2
INX4
E'
INX2
E''
INX4
F
INX2 GFP
TubFlpout >
Inx2 RNAi
F'
INX2
INX4
F''
INX2
F'''
INX4
G
INX2 INX4
TubFlpout
> Inx4 RNAi
G'
INX2
G''
INX4
G'''
INX2
H
CORA RFP
Inx2 clone
H'
RFP
I
***
volume ratio
Control
Inx2
J
ns
surface
Control
Inx2
K
ns
ratio EDU + / total
Control
Inx2

Figure 1

A

tj > RPL10a-GFP (Soma)

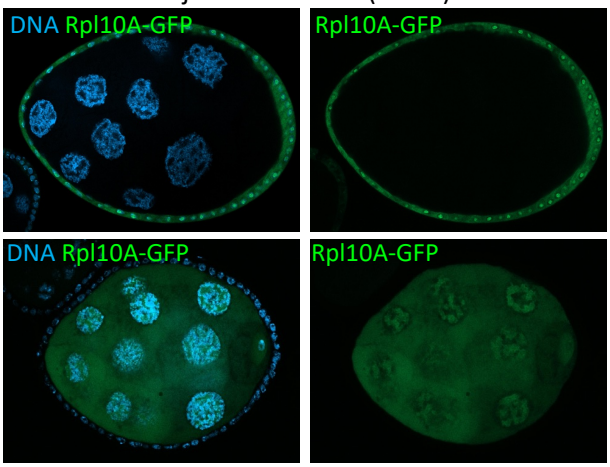

nos > RPL10a-GFP (Germline)

Polysome IP + mRNA Seq

Polysome IP + mRNA Seq

Soma Vs Germline differential expression

B

Soma Vs Germline differential expression	GO Filter	GO analysis	Gene identity
Fold Change >5 *811 genes*	Small molecule metabolic process (GO:0044281) *52 genes (/745)*	Amino acid biosynthesis (GO:0008652) *6 genes (/40)*	*CG10621, CG10623, CG1673, Gs2, GLS, P5CS*
	Transmembrane transporters (GO:0022857) *56 genes (/757)*	Amino acid transporters (GO:0015171) *12 genes (/60)*	*kar, CG15279, CG1628, CG1698, CG16700, NKCC, CG31904, Eaat1, Ncc69, CG43693, CG7888, sbm*

C

Amino acid biosynthesis (GO:008652) *(40 genes)*

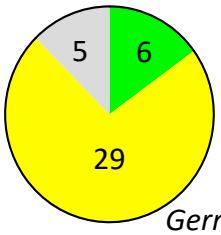

Germline : 0

D

Amino acid transporters (GO:0015171) (*60 genes*)

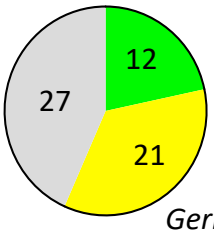

Germline : 0

Soma
Germline
Soma and Germline
not expressed

Figure 2

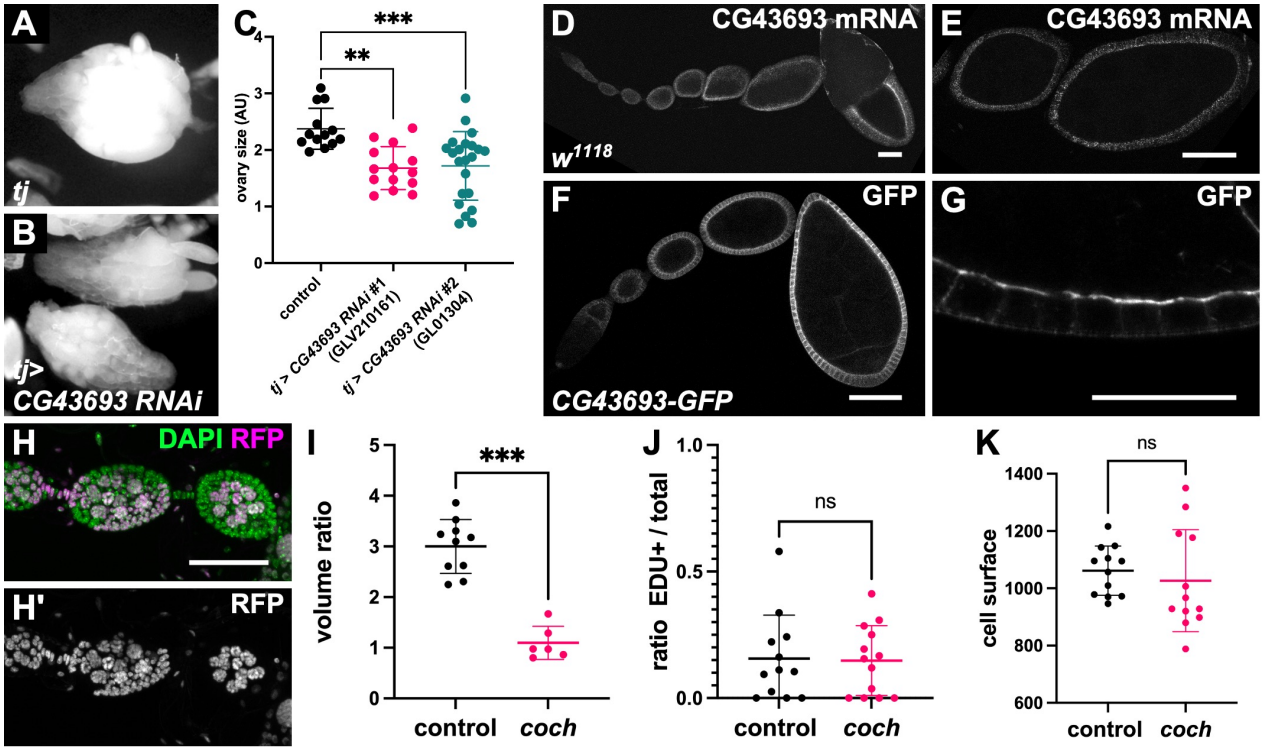
A
tj
B
tj>
CG43693 RNAi
C
***
**
ovary size (AU)
control
tj > CG43693 RNAi #1 (GLV210161)
tj > CG43693 RNAi #2 (GL01304)
D
CG43693 mRNA
w1118
E
CG43693 mRNA
F
GFP
CG43693-GFP
G
GFP
H
DAPI RFP
H'
RFP
I
***
volume ratio
control
coch
J
ns
ratio EDU+ / total
control
coch
K
ns
cell surface
control
coch

Figure 3

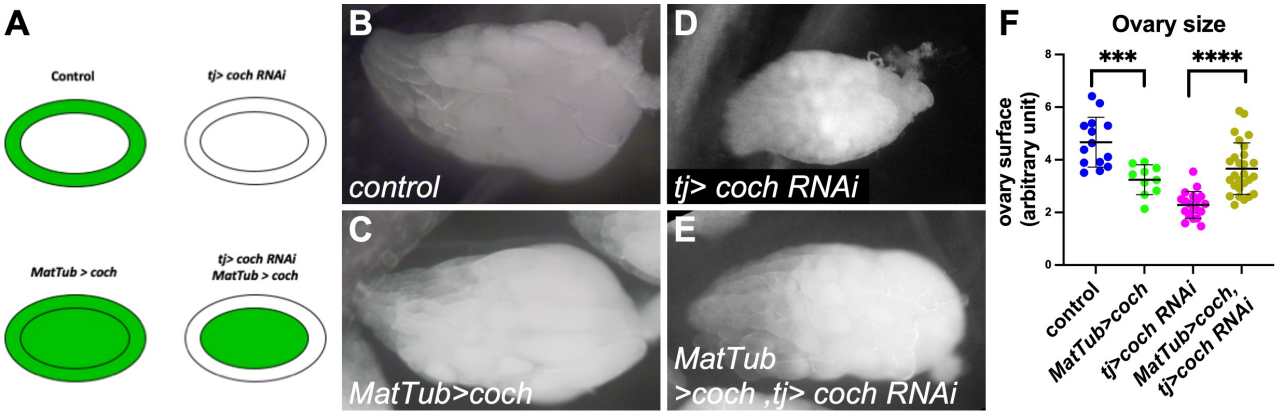
A
Control
tj> coch RNAi
MatTub > coch
tj> coch RNAi
MatTub > coch
B
control
D
tj> coch RNAi
C
MatTub>coch
E
MatTub
>coch ,tj> coch RNAi
F
Ovary size
ovary surface
(arbitrary unit)
***
****
0
2
4
6
8
control
MatTub>coch
tj>coch RNAi
MatTub>coch,
tj>coch RNAi

Figure 4

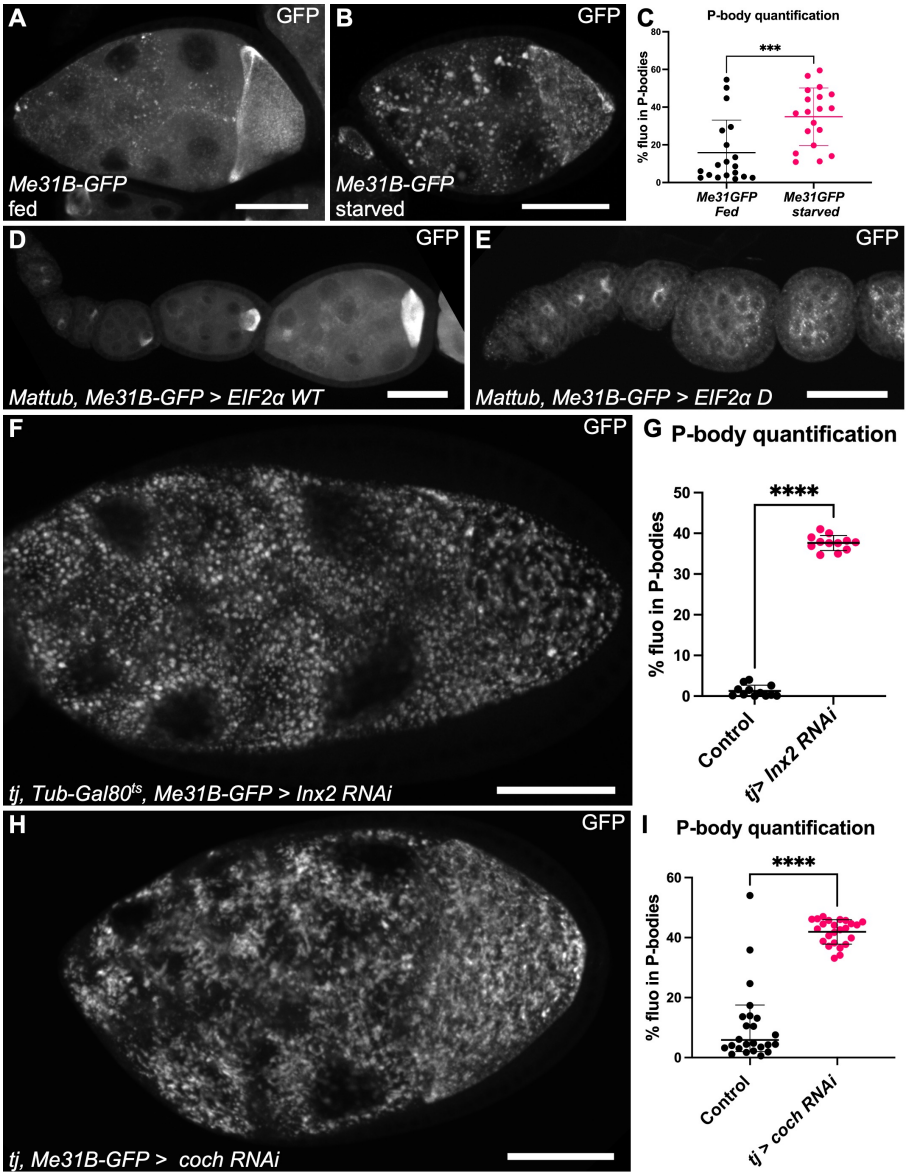
A
GFP
Me31B-GFP
fed
B
GFP
Me31B-GFP
starved
C
P-body quantification
***
% fluo in P-bodies
Me31GFP Fed
Me31GFP starved
D
GFP
Mattub, Me31B-GFP > EIF2α WT
E
GFP
Mattub, Me31B-GFP > EIF2α D
F
GFP
tj, Tub-Gal80ts, Me31B-GFP > Inx2 RNAi
G
P-body quantification
****
% fluo in P-bodies
Control
tj> Inx2 RNAi
H
GFP
tj, Me31B-GFP > coch RNAi
I
P-body quantification
****
% fluo in P-bodies
Control
tj > coch RNAi

Figure 5

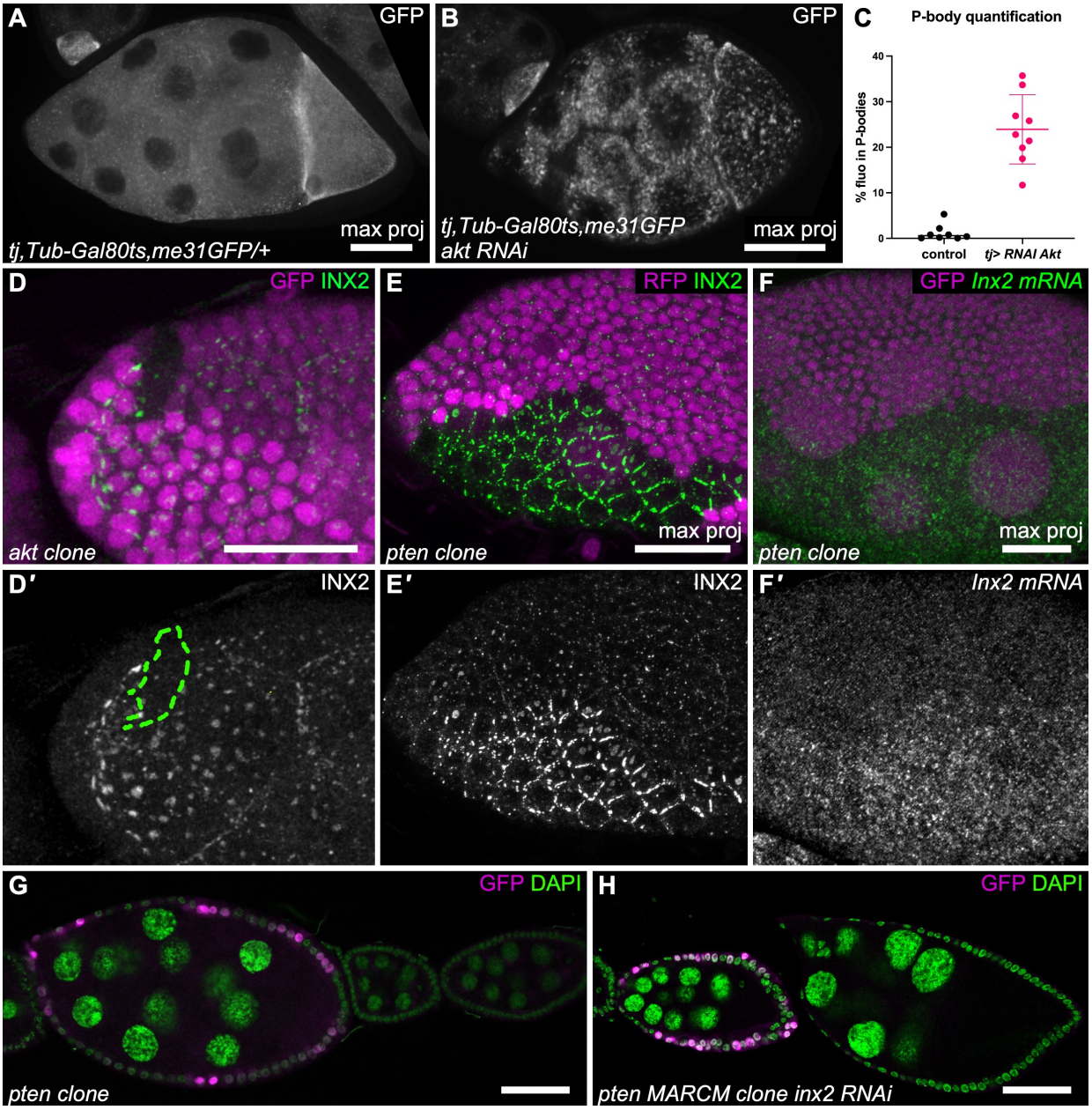
A
GFP
max proj
tj,Tub-Gal80ts,me31GFP/+
B
GFP
tj,Tub-Gal80ts,me31GFP
akt RNAi
max proj
C
P-body quantification
% fluo in P-bodies
40
30
20
10
0
control
tj> RNAI Akt
D
GFP INX2
akt clone
E
RFP INX2
max proj
pten clone
F
GFP Inx2 mRNA
max proj
pten clone
D'
INX2
E'
INX2
F'
Inx2 mRNA
G
GFP DAPI
pten clone
H
GFP DAPI
pten MARCM clone inx2 RNAi

Figure 6

692 **Supplemental data**
693
694 Supplemental data include :
695 - 4 supplemental figures
696 - Table S1 : Excel file of soma vs germline TRAP analysis
697 - Table S2 : Reagents and resources
698 - Table S3 : Genotypes and specific conditions
699
700 **Figure S1:**
701 Maximum intensity projection images of an ovariole after immunostaining for Inx2 (green) and
702 Inx4 (red). Note the progressive increase of Inx2 expression.
703
704 **Figure S2:**
705 Ovariole expressing a QUASP:GFP transgene under the control of the matTub:QF driver.
706
707 **Figure S3:**
708 A,B) Representative images of Me31B-BFP expression in stage 9 follicles from a: A) control
709 female, B) starved control female, C) *gcn2* transheterozygous mutant female, and D protein
710 starved *gcn2* transheterozygous mutant female. E) P-body quantification (fluorescence intensity)
711 in follicles of the indicated genotypes and conditions. Data are the mean ± SD. F,G) Absence of
712 Atf4-GFP protein expression used a read-out of GCN2 activity in F) normal and G) protein-starved
713 conditions. H-I) Ovarioles with germline *gcn2* mutant clones marked by the absence of RFP
714 expression (magenta) and stained for F-actin (green) in H) wild-type background and I) in flies
715 harbouring *coch* RNAi in follicle cells.
716
717 **Figure S4:**
718 A) Coch-GFP expressing follicle with *akt* mutant clones (RFP-negative cells). B) Coch-GFP
719 expressing follicle with flip-out clones that express a constitutively active form of PI3K (RFP-
720 positive cells).
721

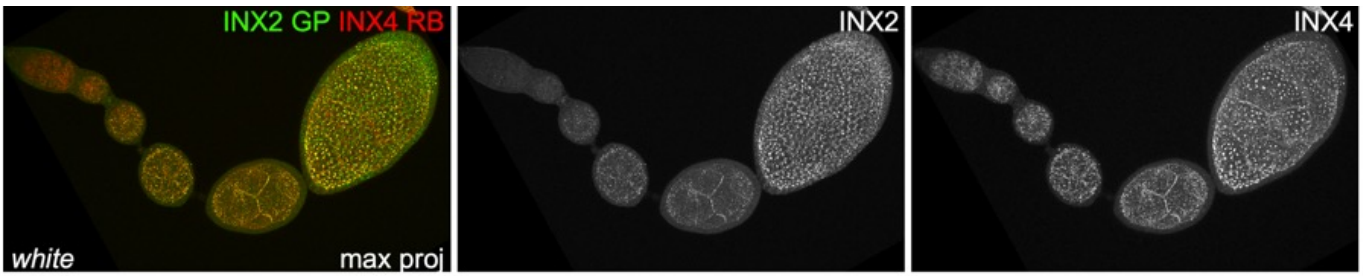

Figure S1

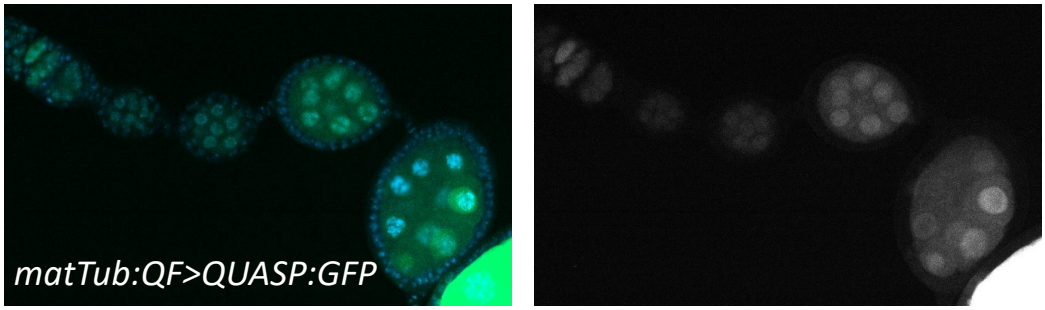

Figure S2

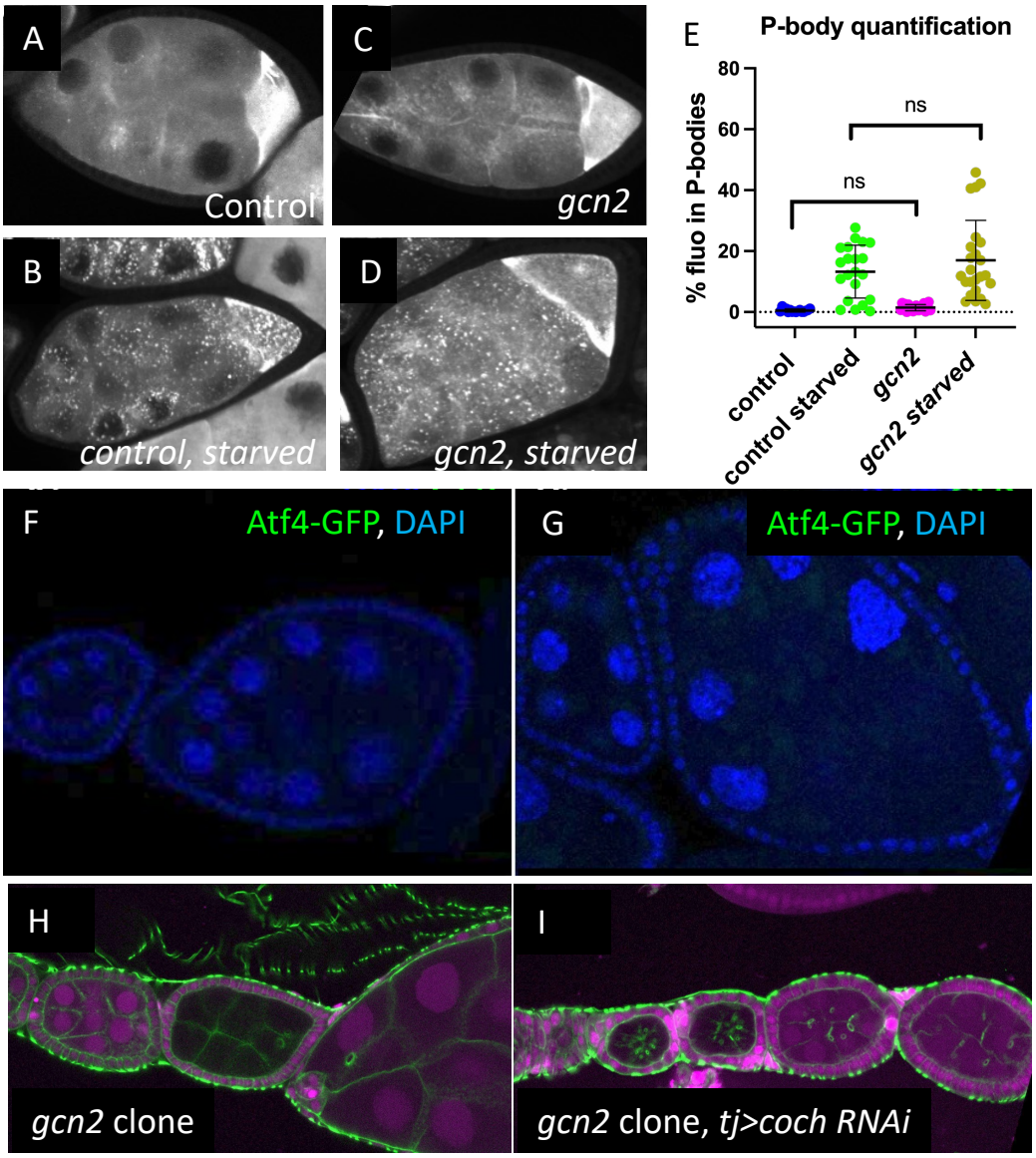
A
Control
C
gcn2
B
control, starved
D
gcn2, starved
E
P-body quantification
% fluo in P-bodies
80
60
40
20
0
ns
ns
control
control starved
gcn2
gcn2 starved
F
Atf4-GFP, DAPI
G
Atf4-GFP, DAPI
H
gcn2 clone
I
gcn2 clone, tj>coch RNAi

Figure S3

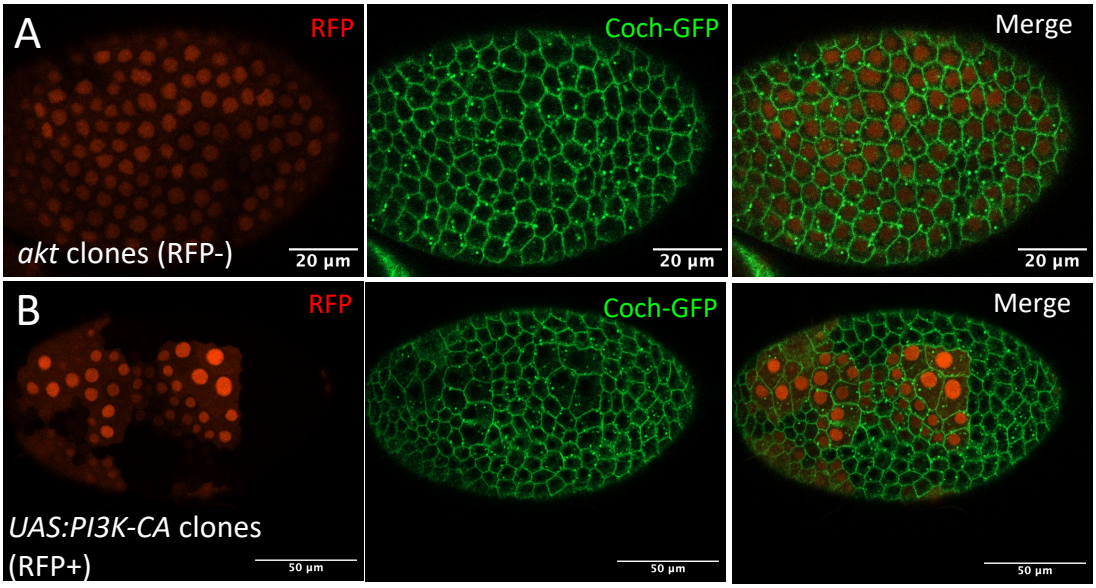
A
RFP
Coch-GFP
Merge
akt clones (RFP-)
20 µm
20 µm
20 µm
B
RFP
Coch-GFP
Merge
UAS:PI3K-CA clones
(RFP+)
50 µm
50 µm
50 µm

Figure S4

722

723 **Table S2: Resources and reagents**

724

RESOURCE OR REAGENT	SOURCE	IDENTIFIER
Experimental models: Organisms/Strains		
tj:Gal4 : P{w+mW.hs=GawB}NP1624	Kyoto Stock Center (DGRC)	FlyBase ID: FBti0034540; DGRC: 104055
FRT19A, Inx2^{A}	Bloomington Drosophila Stock Center	FlyBase ID: FBal0291304; BDSC: 54481
FRT19A, Inx2^{B}	Bloomington Drosophila Stock Center	FlyBase ID: FBal0291305; BDSC: 52363
FRT19A, Inx2^{G0173a}	Bloomington Drosophila Stock Center	FlyBase ID: FBal0151828; DGRC: 111858
UAS :Inx2 RNAi (JF02446)	Bloomington Drosophila Stock Center	FlyBase ID: FBti0128670; BDSC: 29306
UAS : Inx4 RNAi (GL00447)	Bloomington Drosophila Stock Center	FlyBase ID: FBtp0068601; BDSC: 35607
nos:Gal4Vp16	Bloomington Drosophila Stock Center	FlyBase ID: FBti0012410; BDSC: 4937
Mat-tub :Gal4Vp16 (V2H)	Bloomington Drosophila Stock Center	FlyBase ID: FBti0016915; BDSC: 7062
UASp-RPL10a-GFP	Junion G.	Nd
UAS : CG43693 RNAi (GLV21061)	Bloomington Drosophila Stock Center	FlyBase ID: FBti0144657; BDSC: 35696
UAS : CG43693 RNAi (GL01304)	Bloomington Drosophila Stock Center	FlyBase ID: FBti0149385; BDSC: 41873
CG43693/Coch ^{MI01960} : Mi (Michel et al 2005)CG43693^{MI01960}	Bloomington Drosophila Stock Center	FlyBase ID: FBti0132690; BDSC: 34264

Coch/CG43693-EGFP : CG43693 $^{MI01960-GFSTF.0}$	This study	
Me31B-GFP : P{PTT-GB}me31B^{CB05282}	Bloomington Drosophila Stock Center	FlyBase ID: FBal0211797 BDSC: 51530
UASz : eIF2a	This study	
UASz : eIF2a-S51A	This study	
UASz : eIF2a-S51D	This study	
Mat-tub :QF	This study	
QUASp :EGFP	This study	
QUASp :Coch	This study	
UAS :gcn2 sgRNA	Vienna Drosophila Resource Center	VDRC: 341108
nos:Gal4Vp16, ; UAS:Cas9	Bloomington Drosophila Stock Center	BDSC: 54593
FRT gnc2^{CB20}	This study, contains a 2n postion 878 (gg) on gcn2-RA transcript	
FRT gcn2^{CB14}	This study, contains a 1n deletion at position 877 (a) and a 9n insertion (tttccgacc) on gcn2-RA transcript	
4E-BPintron-dsRed	Kang et al, J Cell Biol, 2017	FlyBase ID: FBtp0116205
ATF4-GFP : Mi{PT-GFSTF.1}crcMI02300-GFSTF.1	Bloomington Drosophila Stock Center	FlyBase ID: FBal0314614; BDSC: 59608
FRT40A, Pten^{dj189}	Pan D.	FlyBase ID: FBal0117670
FRT82B, akt^{q}	S. Cohen	Nd
UAS : akt RNAi (HM04007)	Bloomington Drosophila Stock Center	FlyBase ID: FBti0130466 BDSC 31701
UAS : PI3K-CA (Chromosome II)	This study, obtained by P-element mobilization of UAS:PI3K92E-CAAX (FBal0156077)	
Antibodies		

anti-Inx4, rabbit	G. Tanentzapf	1/2000
anti-Inx2, Guinea Pig	G. Tanentzapf	1/400
anti-Inx2 rabbit	P. Phelan	1/5000
anti-coracle mouse	DSHB	C615.16 1/100
anti-mouse –Alexa 488	Life technologies	A21202 1/1000
anti-rabbit -Cy5, Donkey	Jackson Immunoresearch	711-175-152 dilution 1/1000
Anti-rabbit pig-Cy3, Donkey	Jackson Immunoresearch	711-165-152 dilution 1/1000
anti-guinea pig-Cy5, Donkey	Jackson Immunoresearch	703-175-155; dilution 1/1000
Anti-guinea pig-Cy3, Donkey	Jackson Immunoresearch	706-165-148 dilution 1/1000
Chemicals, Peptides, kits		
Phalloidin Atto-488, -550, -633	Sigma	#49409, #19083, #68825
DAPI	Sigma	100 µg/ml D8417-1MG
EdU Click-iT™ Plus Alexa 555	Thermo Fisher	C10638
Ovation 1-16 droso Universal RNA-seq kit	Nugen	No longer distributed
Software and Algorithms		
Fiji	(Schindelin et al, 2012)	
Prism		

725

726

727 **Table S3: Genotypes and specific conditions**

728 (h: hours; HS: heat-shock, GP : grape juice agar plate)

729

Figure	Genotype	Condition
Figure 1 BE	*w^{1118}*	25°C
F	*y,w,hs:flp122; Act5C:FRT-Stop-FRT-Gal4, UAS:GFP , UAS:Inx2 RNAi*	1HS, 4 days at 30°C
G	*y,w,hs:flp122; Act5C:FRT-Stop-FRT-Gal4, UAS:GFP , UAS:Inx4 RNAi*	1HS, 4 days at 30°C
H,I	*FRT19A, Inx2 / FRT19A, Ubi:nlsRFP, hs:flp122*	1HS, 10-12 days at 25°C
J,K	*FRT19A, Inx2 / FRT19A, Ubi:nlsRFP, hs:flp122*	1HS, 2 days at 25°C
Figure 2 A	*tj:Gal4 / UASp :Rpl10a-GFP and UASp :Rpl10a-GFP; nos:Gal4VP16*	25°C
Figure 3 A	*tj:Gal4*	4 days at 30°C
B	*tj:gal4 / UAS: CG43693 RNAi ^{GL01304}*	4 days at 30°C
C	*tj:Gal4*	4 days at 30°C
	tj:gal4 / UAS: CG43693 RNAi^{GLV210161}	
	tj:gal4 / UAS: CG43693 RNAi^{GL01304}	
D,E	*w^{1118}*	25°C
F,G	*CG43693-GFP (or coch-GFP)*	25°C
H,I	*y,w,hs:flp122; FRT2A, coch^{MI01960}/ FRT2A, Ubi:nlsRFP*	2HS, 8 days at 25°C
J,K	*y,w,hs:flp122; FRT2A, coch^{MI01960}/ FRT2A, Ubi:nlsRFP*	1HS, 2 days at 25°C
Figure 4	*tj:gal4, matTub:QF, / +*	4 days at 30°C
A,B,F	*tj:gal4, matTub:QF,; QUASP:coch*	
A,C,F	*tj:gal4, matTub:QF,; UAS: coch RNAi^{GLV21061}*	
A,D,F	*tj:gal4, matTub:QF, QUASP:coch; UAS: coch RNAi^{GLV21061}*	
A,E,F		
Figure 5	*Me31B-GFP*	25°C
A,C	*Me31B-GFP*	25°C, 14h on GP
C		25°C
D	*matTub :Gal4Vp16, Me31B-GFP , UASz: eIF2α*	25°C
E,F	*matTub :Gal4Vp16, Me31B-GFP, UASz: eIF2α-S51D*	18°C, 14h at 30°C
G,H	*tj:gal4,Tub:Gal80^{ts},Me31B-GFP / UAS:Inx2RNAi*	2 days at 25 °C
	tj:gal4, Me31B-GFP / UAS: coch RNAi^{GLV21061}	
Figure 6 A,C	*tj:Gal4, Tub:Gal80^{ts} Me31B-GFP*	2 days at 30°C
B,C	*tj:Gal4, Tub:Gal80^{ts,} Me31B-GFP / UAS: akt RNAi*	2 days at 30°C
D	*y,w,hs:flp122; FRT82B, akt^{q} / FRT82B, Ubi:GFP*	1HS, 4 days at 25°C

E,F	*y,w,hs:flp122 ; FRT40A,Pten^{dj189} / FRT40A, Ubi:nlsRFP*	1HS, 4 days at 25°C
G	*y,w,hs:flp122, Tub:Gal4, UAS :GFP ; FRT40A,Pten^{dj189} / FRT40A, Tub :Gal80*	1HS, 5 days at 25°C 1HS, 6 days at 25°C
H	*y,w,hs:flp122, Tub:Gal4, UAS :GFP ; FRT40A,Pten^{dj189} / FRT40A, Tub :Gal80; UAS :Inx2 RNAi*	1HS, 6 days at 25°C
Figure S1	*w^{1118}*	25°C
Figure S2	*MatTub:QF / QUASP:GFP*	25°C
Figure S3 A,C	*Me31B-GFP*	25°C
B,C	*Me31B-GFP, gcn2^{CB20}/ gcn2^{CB14}*	25°C
D,E	*ATF4-GFP*	25°C
H	*y,w,hs:flp122 ; FRT82B, gcn2^{CB14} / FRT82B, Ubi:nlsRFP*	1HS, 5 days at 30°C
I	*y,w,hs:flp122 ; tj :Gal4 ; UAS: coch RNAi^{GL01304}, FRT82B, gcn2^{CB14} / FRT82B RFP*	1HS, 5 days at 30°C
Figure S4 A	*y,w,hs:flp122 ; coch-GFP, FRT82B, akt^{q} / FRT82B, Ubi:nlsRFP*	1HS, 5 days at 25°C
B	*y,w, hsflp122; Act5C:FRT-STOP-FRTGal4; UAS:RFP/ UAS:PI3K-CAAX ; coch-GFP*	1HS, 5 days at 25°C

730

731